

Origins of Protein Denatured State Compactness and Hydrophobic Clustering in Aqueous Urea: Inferences from Nonpolar Potentials of Mean Force

Seishi Shimizu and Hue Sun Chan*

Protein Engineering Network Centres of Excellence, Department of Biochemistry and Department of Medical Genetics and Microbiology, Faculty of Medicine, University of Toronto, Toronto, Ontario, Canada

ABSTRACT Free energies of pairwise hydrophobic association are simulated in aqueous solutions of urea at concentrations ranging from 0–8 M. Consistent with the expectation that hydrophobic interactions are weakened by urea, the association of relatively large nonpolar solutes is destabilized by urea. However, the association of two small methane-sized nonpolar solutes in water has the opposite tendency of being slightly strengthened by the addition of urea. Such size effects and the dependence of urea-induced stability changes on the configuration of nonpolar solutes are not predicted by solvent accessible surface area approaches based on energetic parameters derived from bulk-phase solubilities of model compounds. Thus, to understand hydrophobic interactions in proteins, it is not sufficient to rely solely on transfer experiment data that effectively characterize a single nonpolar solute in an aqueous environment but not the solvent-mediated interactions among two or more nonpolar solutes. We find that the m -values for the rate of change of two-methane association free energy with respect to urea concentration is a dramatically nonmonotonic function of the spatial separation between the two methanes, with a distance-dependent profile similar to the corresponding two-methane heat capacity of association in pure water. Our results rationalize the persistence of residual hydrophobic contacts in some proteins at high urea concentrations and explain why the heat capacity signature (ΔC_p) of a compact denatured state can be similar to ΔC_p values calculated by assuming an open random-coil-like unfolded state. *Proteins* 2002; 49:560–566. © 2002 Wiley-Liss, Inc.

Key words: hydrophobicity; urea denaturation; solvent accessible surface area; compact denatured states; m -value; heat capacity

INTRODUCTION

The denaturing property of urea is exploited routinely to study protein energetics.^{1–4} A long-standing approach to quantitate its effects is through transfer free energies deduced from solubility measurements of amino acid derivatives and related model compounds.^{5–10} Group additivity is often assumed, whereby the contribution of a chemi-

cal group is related to its solvent exposure calculated using “fractional exposure” parameters^{2,5} or geometric measures such as solvent accessible surface area (SASA).¹¹ From these analyses, it has been recognized early on that the denaturing action of urea involves *both* the amino acid side-groups and the main-chain peptide groups of a protein.^{5,9,11–14} The scope of the present investigation is limited to urea’s effects on hydrophobicity.

Physical pictures based on transfer free energies are useful but far from complete. For instance, although in such perspectives chemically denatured states of proteins are often assumed to be open and random-coil-like,^{2,5,11,15} there is mounting evidence that the urea-denatured states of some proteins are incompletely disordered, with residual hydrophobic clustering^{16–19} and even elements of native-like topology²⁰ (see also refs. 21 and 22). Contrary to the expectation that increasing concentration of chemical denaturants leads to a general nonspecific weakening of hydrophobic interactions^{5,23} and thus should always render protein conformations less compact, small-angle X-ray scattering (SAXS) indicates no significant postdenaturation expansion of the urea- or GuHCl-denatured states of several proteins with further addition of denaturant.²⁴ Certain nonlocal structural elements of $\Delta 131\Delta$ also show little variation when urea concentration is increased from 0 to 8 M.²⁰

To put these puzzles in an appropriate perspective, it is crucial to realize that transfer experiments parameterize “bulk” but not “pair” hydrophobic interactions.²⁵ They effectively compare a single model compound solute in (1) an aqueous solvent versus in (2) a nonpolar solvent such as liquid alkanes or octanol. These situations presumably correspond to the model compound being (1) part of an open denatured state and (2) completely buried in the hydrophobic core of a folded protein.²⁶ As such, these measurements are intrinsically ill-equipped to tackle interactions in compact denatured states, which likely involve contacting hydrophobic groups that are at the same time partially solvated. Free energies for such interactions,

*Correspondence to: Hue Sun Chan, Department of Biochemistry, University of Toronto, Medical Sciences Building, 5th Fl., 1 King’s College Circle, Toronto, Ontario M5S 1A8, Canada. E-mail: chan@arrhenius.med.toronto.edu

Received 19 July 2002; Accepted 30 July 2002

which are not directly probed by transfer experiments, are nonetheless often modeled using transfer data by assuming simple proportionality relations between solvation free energy and SASA or other geometric measures. Understandably, skepticism toward such treatments was raised^{27,28} soon after the seminal theory of Pratt and Chandler²⁹ in 1977 on the potential of mean force (PMF) between two nonpolar solutes because SASA does not predict the PMF's spatial dependence. Size dependence^{30,31} deserves closer examination as well: While the solubilities of larger hydrophobic amino acids such as leucine and phenylalanine increase with urea concentration, the solubility of alanine, which has a small nonpolar group, shows the opposite trend.⁵ It follows that presupposing a generic diminishing of hydrophobic interactions by urea may not be adequate. We address these questions below by investigating solubilities and pairwise PMFs of nonpolar solutes in aqueous urea solvents.

SIMULATION METHODS AND RATIONALE

Hydrophobic PMFs cannot be directly determined by current experimental techniques. Computer simulations are thus essential.^{32–38} Two-methane PMF in aqueous urea was first calculated at 6 M by Wallqvist et al.,³⁹ who concluded that urea stabilizes hydrophobic association. This conclusion was subsequently corroborated by 7-M simulations of Ikeguchi et al.⁴⁰ Building on these pioneering studies, we now consider a wider range of urea concentrations systematically. Starting with configurations we obtained from appropriate preequilibration runs, constant-pressure (*NPT*) Monte Carlo simulations are performed here at 298 K under atmospheric pressure in periodic boxes of size $\approx 23 \times 23 \times 23 \text{ \AA}^3$ containing 396 solvent molecules (unless otherwise specified) using the software BOSS Version 4.1.⁴¹ The urea concentrations and the number of all-atom model urea molecules and TIP4P waters in our simulations (first and second entries in curly brackets, respectively) are: 0 M {0, 396}, 2 M {15, 381}, 4 M {32, 364}, 5.5 M {45, 351}, 6 M {51, 345}, and 8 M {73, 323}. Interactions are truncated at 9.0 \AA , as in Wallqvist et al.,³⁹ except for the interactions between solvent molecules and neopentane-like nonpolar solutes (referred to as “neopentanes” below) that we truncate at 12.0 \AA . Neopentane is studied here as an example of larger hydrophobic groups. It is modeled by a Lennard–Jones sphere with size and interaction parameters defined by Kuharski and Rossky.⁴²

The single-methane solvation free energies in Figure 1(A) are calculated by the test-particle insertion method.^{36,37,43} Aqueous urea solvents are first equilibrated over 1.3×10^5 Monte Carlo passes. Snapshots of coordinates are then collected every 100 passes over the next 4.0×10^6 passes for all urea concentrations studied except 6.2×10^7 passes are used for the 0-M (pure water) case.⁴⁴ Then, 10,000 attempted solute insertions are performed per snapshot. Methane–methane (Fig. 2) and neopentane–methane PMFs [Fig. 3(A)] are also computed by the test-particle method. In either case, a methane or neopentane is placed at the center of the solvent box. Snapshots of the coordinates are taken

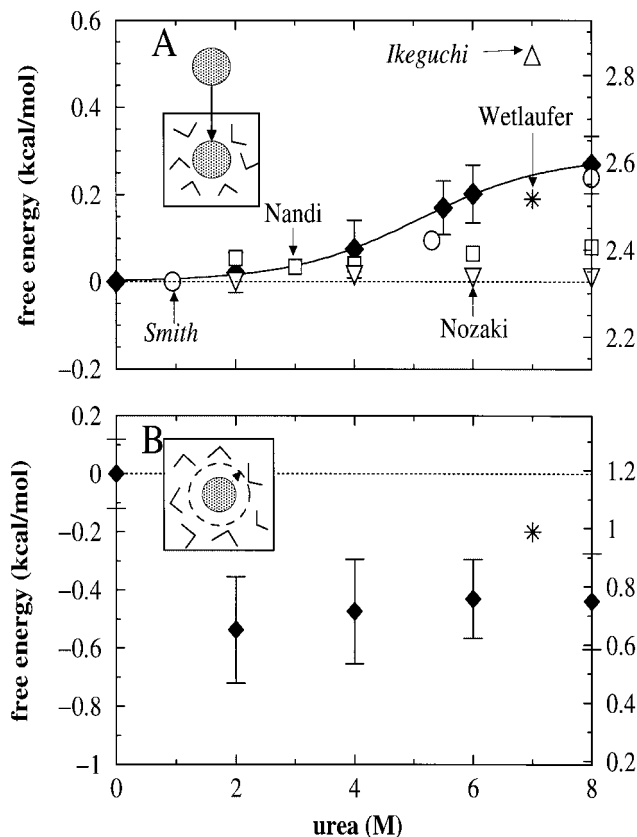


Fig. 1. Solvation free energy of a single (A) methane and (B) neopentane as functions of aqueous urea concentration. Present results (solid diamonds) are obtained by (A) test-particle insertion and (B) free energy perturbation, as illustrated by the inset cartoons wherein shaded circles represent methane or neopentane and V shapes represent the aqueous urea solvent. Free energies of transfer from pure water to aqueous urea (left scales) are the differences between the computed absolute solvation free energies (vacuum to aqueous urea, right scales) and the computed vacuum to water free energy (dotted horizontal lines). Error bars are for absolute solvation free energies. Direct experimental measurement data from Wetlaufer et al.,⁶ experimental estimates from refs. 5 and 9, and previous theoretical predictions from refs. 40 and 45 for water to aqueous urea transfer free energies under the same conditions (symbols labeled respectively by “Wetlaufer,” “Nozaki,” “Nandi,” “Smith,” and “Ikeguchi”) are included for comparison. (A) The continuous curve through our simulated data points is a guide for the eye. Error bars show the range between the minimum and maximum values observed among the last 50 cumulative averages taken at interval of 19,200 passes during the simulation.³⁷ The uncertainty of methane hydration free energy in pure water so determined is ± 0.006 kcal/mol. (B) Neopentane free energies are obtained by perturbatively converting a methane into a neopentane. Ten perturbation steps are used, each consisting of no less than 2.0×10^4 equilibration passes followed by at least 2.0×10^6 sampling passes. Error bars correspond to the sum, over all perturbation steps, of standard deviations of block averages covering 1.26×10^3 passes each.

every 100 passes during equilibrium sampling. Subsequently, 20,000 attempts to insert a methane at different positions are made per snapshot.^{36,44} Because of neopentane's relatively large size, the test-particle method is not practical for the determination of single-neopentane solvation free energies [Fig. 1(B)] and two-neopentane PMFs [Fig. 3(B)]. These quantities are calculated by free energy perturbation approaches that either convert a methane into a neopentane or translate a neopentane spatially.

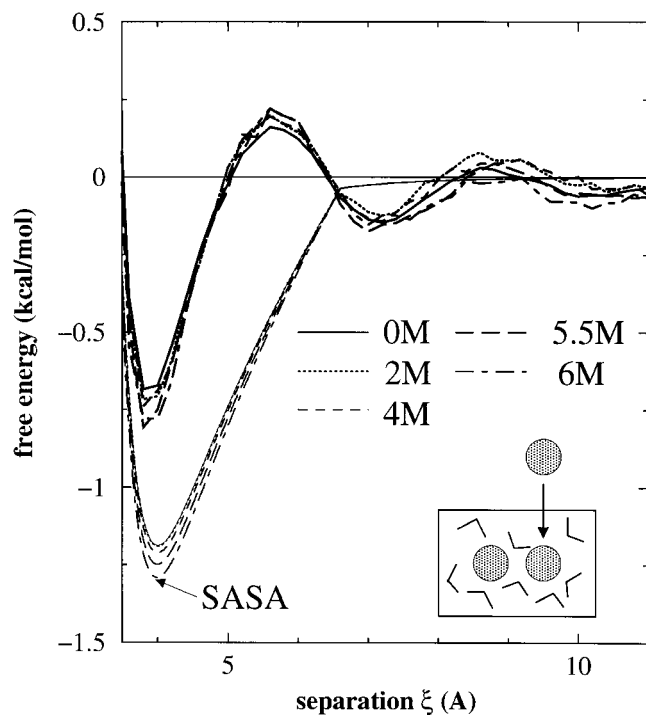


Fig. 2. Methane–methane PMFs in five different concentrations of aqueous urea (line styles as indicated); ξ is the distance between the centers of mass of the two methanes. SASA predictions are included for comparison (see text). For each nonzero urea concentration, at least 1.2×10^6 equilibrating passes are run before 2.9×10^7 sampling passes are used to obtain configurations for test-particle insertions.

TRANSFER DATA DO NOT ACCURATELY PREDICT PAIRWISE INTERACTIONS

Our simulation results in Figure 1(A) show that urea decreases the aqueous solubility of methane. Single-methane solvation free energy apparently has a sigmoidal dependence on urea concentration, with most of the free energy increase (methane becoming less soluble) taking place around 3–6 M. This is in good agreement with a direct experimental measurement of methane gas solubility in 7 M urea by Wetlaufer et al.⁶ and the SPC/E simulations of Smith.⁴⁵ In contrast, Ikeguchi et al.’s⁴⁰ TIP3P prediction is more than double the experimentally determined value, suggesting that large errors might have accumulated in their particle growth calculation. Figure 1(A) also shows water to aqueous urea transfer free energies of alanine side-chain, deduced by Nozaki and Tanford⁵ and Nandi and Robinson⁹ from solubility data of amino acid derivatives. These contributions are based on group additivity assumptions. Hence, they do not necessarily agree with methane solvation free energies, although it is noteworthy that they share the same positive sign. Solubilities of cyclic dipeptides in aqueous urea were measured by Zou et al.¹⁰ If group additivity was assumed, the differences between their alanine–alanine and alanine–glycine free energy data would lead to slightly negative contributions of -0.002 to -0.005 kcal/mol upon transferring an alanine side-chain from pure water to 0.5–3 M urea.

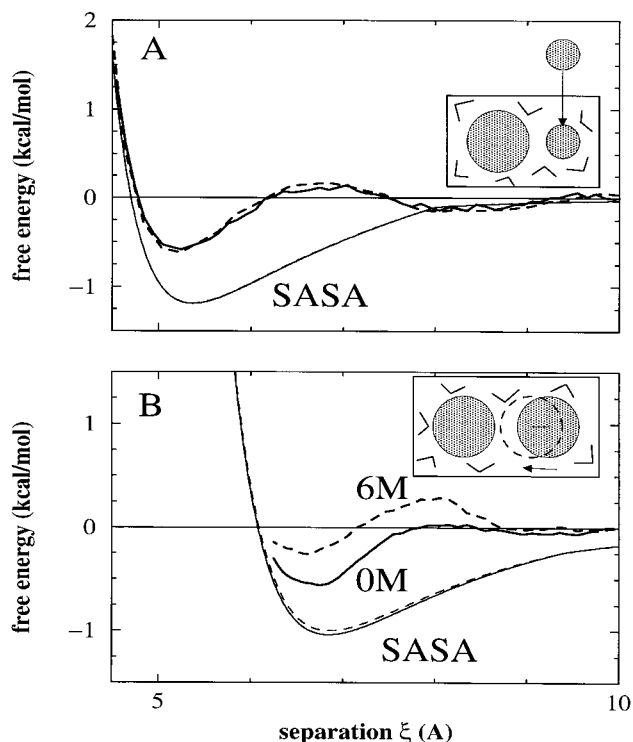


Fig. 3. Neopentane–methane (A) and neopentane–neopentane (B) PMFs in pure water (0 M, solid curves) and 6 M aqueous urea (broken curves) are determined by methods outlined in the text; ξ is center-of-mass separation. Here, the SASA-predicted PMFs are obtained with γ defined as the simulated solvation free energy of a single neopentane [Fig. 1(B)] divided by its SASA. (A) Snapshots for test-particle insertions are collected over 1.1×10^7 and 3.7×10^7 passes, respectively, for 0 and 6 M, after 1.3×10^5 equilibration passes for each case. (B) A larger simulation box of $\approx 25 \times 25 \times 37 \text{ \AA}^3$ is used for the free energy perturbation calculation (730 water molecules for 0 M, 636 water molecules and 94 urea molecules for 6 M), where the larger dimension is along ξ . The perturbative step (double-wide sampling) equals 0.05 \AA change in ξ and PMFs are taken to be zero at $\xi = 10 \text{ \AA}$. At each step, 1.2×10^6 passes are used for averaging, which are preceded by no less than 3.0×10^4 equilibration passes.

However, the trend exhibited by methane in Figure 1(A) is not shared by all nonpolar solutes. Figure 1(B) shows that neopentane prefers to be in aqueous urea than in pure water, although the free energy of transfer appears to be insensitive to the variation of urea concentration between 2–8 M [Fig. 1(B)]. This prediction is qualitatively consistent with the direct experiment of Wetlaufer et al.⁶ A simulated neopentane transfer free energy close to the experimental value was reported by Ikeguchi et al.,⁴⁰ but they used a neopentane Lennard–Jones well depth of $\epsilon = 1.00$, significantly different from the $\epsilon = 0.8351$ adopted here from Kuharski and Rossky.⁴² The opposing trends in Figures 1(A) and 1(B) underscores the importance^{46,47} of nonpolar solute size in urea-modulated hydrophobicity.

Figure 2 shows that urea does not always weaken hydrophobic interactions. To the contrary, contact interaction between two methanes and their solvent-separated PMF minimum are slightly stabilized by urea. These findings are in qualitative agreement with Wallqvist et al.³⁹ and Ikeguchi et al.⁴⁰ The SASA-predicted PMFs in

Figures 2 and 3 are the sum of the direct Lennard–Jones interaction between the two nonpolar solutes and a ξ -dependent solvation contribution that equals to $\gamma[\text{SASA}(\xi) - (\text{SASA})_1 - (\text{SASA})_2]$, where $\text{SASA}(\xi)$, $(\text{SASA})_1$, and $(\text{SASA})_2$ are, respectively, the SASA of the two solutes and first and second solute in isolation. For the two-methane case in Figure 2, $(\text{SASA})_1 = (\text{SASA})_2$ and γ is equal to the simulated single-methane solvation free energy for a given urea concentration [Fig. 1(A)] divided by $(\text{SASA})_1$. Figure 2 shows that the favorability of two-methane association is drastically overestimated by SASA.^{36,44}

UREA ACTION DEPENDS ON THE SIZES OF HYDROPHOBIC SOLUTES

We now consider pairwise hydrophobic interactions involving larger nonpolar solutes. Figure 3(A) shows that the interaction between a neopentane and a methane in aqueous urea is similar to that between two methanes (Fig. 2). In both cases, the contact interaction in pure water is not destabilized by the addition of 6 M urea. Based on a similar result, Wallqvist et al. commented that “for these model systems urea appears to enhance the hydrophobic interaction and acts as a renaturant.”³⁹ However, urea-enhanced hydrophobic interactions is not a general phenomenon for nonpolar solutes of all sizes. Figure 3(B) indicates that, in contrast, the neopentane–neopentane contact interaction is destabilized by $\approx +0.30$ kcal/mol when the solvent is changed from pure water to 6 M aqueous urea. This effect is much more pronounced than the corresponding SASA prediction based upon single-neopentane solvation data. We emphasize, however, that because the test-particle method is not used, unlike the calculations in Figures 2 and 3(A), the zero-PMF baselines in Figure 3(B) may involve considerable uncertainties.^{36,44} To address this question, we also performed independent perturbation calculations in 396-solvent boxes (as specified above) that convert a neopentane–methane pair [Fig. 3(A)] to a neopentane–neopentane pair at $\xi = 6.6$ Å. These provide neopentane–neopentane contact PMF estimates of ≈ -0.48 and $+0.25$ kcal/mol for 0 and 6 M, respectively, implying a destabilization of as much as $+0.73$ kcal/mol by 6 M urea. These considerations lead us to expect the present prediction of significant urea-induced destabilization of pairwise neopentane hydrophobic interactions to be robust. Recalling that at the single-solute level (Fig. 1) urea weakens the hydrophobicity of larger nonpolar solutes but enhances that of smaller nonpolar solutes,^{6,40,46,47} it is noteworthy that a similar heuristic trend of nonpolar solute size dependence may hold also at the two-solute level.

CONFIGURATION-DEPENDENT m -VALUES AND HEAT CAPACITY

The overall trend of urea-dependent two-methane interactions is highlighted by Figure 4(A). This analysis of ξ -dependent m -values is useful although two-methane free energies are not in general linear in urea concentration. Figure 4(A) shows that a pair of contacting methanes is stabilized by urea [$m(\xi) < 0$ for $\xi = 3.8$ Å; cf. Fig. 2],

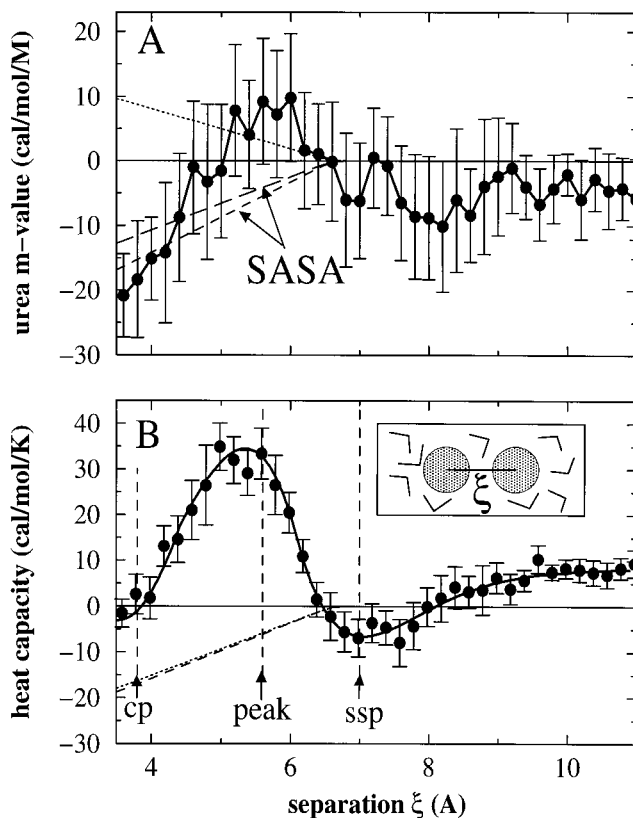


Fig. 4. Configuration-dependent two-methane m -value and heat capacity. Error bars for simulation results (solid circles) are calculated by the procedure described in Figure 1 of ref. 37. The solid curve in (B) serves as a guide for the eye. The vertical broken lines labeled “cp,” “peak,” and “ssp” mark the approximate positions, respectively, of the two-methane contact pair, desolvation barrier, and solvent-separated minimum of the PMFs in Figure 2. (A) The urea m -value $m(\xi)$ is obtained by fitting the two-methane PMFs for the five urea concentrations [urea] in Figure 2 at the given ξ to a linear relation $A(\xi) + m(\xi)[\text{urea}]$, where $A(\xi) \approx$ PMF in pure water. (B) The heat capacity change $\Delta C_p(\xi)$ upon bringing two methanes initially infinitely far apart to a separation ξ in pure water under atmospheric pressure is computed by simulations at eight different temperatures, as described in ref. 37. The present $\Delta C_p(\xi)$ is based on more extensive simulation data than that used for an essentially identical result in ref. 37. Here, 6.2×10^7 and 1.4×10^7 Monte Carlo passes are used for 298 and 278 K, respectively, and at least 4.0×10^6 passes are used for the other six temperatures. Simulation results are compared with SASA predictions as follows. *Dotted lines*: SASA predictions are based on the average hydrophobic residue parameters derived by Myers et al.³ from protein data (eqs. 11 and 9 in ref. 3); the *long dashed line* in (A) is calculated using SASA and based on experimental transfer data of Wetlaufer et al. [see Fig. 1(A)]; *broken lines*, these $m(\xi)$ and $\Delta C_p(\xi)$ SASA predictions are based, respectively, on our simulated single-methane solvation data in Figure 1 and the simulated single-methane hydration heat capacity obtained from hydration free energies at eight different temperatures.³⁷

contrary to the destabilization predicted by conventional analyses of protein stability data (dotted line). Presumably this is because parameters in the latter analyses are effectively derived mostly from urea effects on the main-chain and larger hydrophobic side-groups. Interestingly, Figure 4(A) shows that to a limited degree two-methane $m(\xi)$ -values are accountable by single-methane transfer data (broken and long broken lines). Here, single-methane m -values are calculated from linear approximations of the

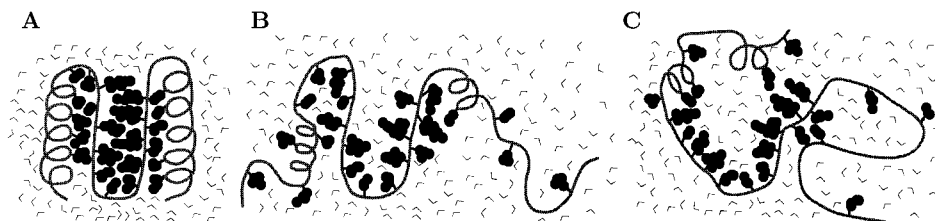


Fig. 5. A physical picture of denatured proteins. (A) Schematics of a protein native structure. Solvent is mostly excluded from its hydrophobic core. (B, C) Examples of denatured state conformations that are not completely open but are relatively compact, with fluctuating and loosely formed hydrophobic contacts, most of which are partially exposed to solvent.

urea dependencies of simulated and experimental solvation free energies in Figure 1(A). Based on these, although SASA fails to account for the positive two-methane $m(\xi)$ -values in the PMF desolvation barrier region ($\xi \approx 5.7$ Å), SASA quite accurately predicts the negative $m(\xi)$ -values for two methanes in contact or close to being so ($\xi \approx 4$ Å). This suggests that the mechanism for urea-induced stabilization of a contacting methane pair [Fig. 4(A)] may be intimately related to the reduction of methane solubility by urea [Fig. 1(A)].

Bulk-phase transfer data indicates that hydrophobic burial is associated with a decrease in heat capacity ($\Delta C_p < 0$); thus, protein conformational changes are often characterized by ΔC_p .⁴⁸ For example, based on protein stability data, Myers et al.³ estimated that $\Delta C_p \approx -0.28$ cal/mol/K per Å² reduction in nonpolar SASA. An essentially identical value of -0.29 cal/mol/K/Å² can be obtained by dividing our simulated heat capacity of a single methane (40 cal/mol/K in pure water) by its SASA. However, Figure 4(B) shows that these presumed ΔC_p – SASA proportionality relations fail to account for the directly simulated two-methane heat capacity.³⁷ When two methanes move toward each other, instead of a monotonic decrease in heat capacity resulting from SASA reduction, Figure 4(B) exhibits a dramatic nonmonotonic profile that shares some similarity with the m -value profile in Figure 4(A). Contrary to conventional expectation, the heat capacity signature of two isolated methane-sized solutes in water ($\Delta C_p(\xi) \rightarrow 0$ as $\xi \rightarrow \infty$) is essentially indistinguishable from that when they are in contact ($\Delta C_p(\xi) \approx 0$ for $\xi = 3.8$ Å).³⁷

A PHYSICAL SCENARIO OF COMPACT DENATURED STATES

Our focus here is on the subtle complexity of pairwise hydrophobic interactions vis-à-vis the relative simplicity of transfer-based single-solute (i.e., “bulk”; see ref. 25) hydrophobic effects. Other interaction types important for protein folding such as urea-modulated polar interactions^{5,39} and charge interactions (see, e.g., ref. 49) are not investigated. As well, even two-solute considerations cannot offer a complete picture because solvent-mediated interactions are known to deviate from pairwise additivity.⁴⁴ Indeed, certain protein thermodynamic and kinetic behaviors may well arise from many-body effects that include a cooperative interplay between local and nonlocal

interactions.⁵⁰ However, notwithstanding the obvious limitations of the present study, we find that several puzzling phenomena of compact denatured states may be tentatively rationalized by an understanding of pairwise hydrophobic interactions.

The denatured states of several proteins have been found to be relatively compact by SAXS at high temperatures or under high concentrations of urea or Gu-HCl.^{24,51,52} Their radii of gyration (R_g) are only $\approx 2/3$ of the corresponding random-coil values from rotational isomeric state theory for the polypeptide chains.⁵³ Specific residual structures and hydrophobic clustering have also been detected in denatured states.^{16–20,54,55} These observations contributed to the recent suggestion⁵⁶ that steric effects⁵⁷ and local structure propensities may encode nonlocal (long-range) protein structures. Excluded volume effects do reduce the number of accessible conformations relative to the hypothetical situation when all or part of such effects are neglected.⁵⁷ But, even when excluded volume effects are fully taken into account, in the absence of interactions that favor compactification and folding, the number of accessible conformations still grows exponentially with chain length.⁵⁸ This is most apparent from a recent set of extensive simulations of natural proteins with up to $N \approx 150$ amino acid residues wherein intrachain atomistic steric effects are explicitly accounted for,⁵⁹ in which the number of main-chain (C_α) conformations is estimated to vary approximately as μ^N , with $\mu \approx 1.3$ – 2.9 , consistent with an earlier estimate of $\mu \approx (4118/1600) = 2.57$.⁶⁰ Together, these considerations imply that while local steric effects are important, hydrophobic and other compactification forces are needed to address compactness and hydrophobic clustering in protein denatured states.

The physical scenario we propose for compact denatured states is illustrated by Figure 5, which may also be partially applicable to molten-globule-like states.⁶¹ Qualitatively, the discussion above suggests that, as a part of its denaturing action in addition to its effect on the peptide backbone,^{5,39} urea disrupts [Fig. 1(B)] the packing of, or weakens [Fig. 3(B)], the native contacts between relatively big nonpolar groups [Fig. 5(A)]. The dissociation of well-packed hydrophobics may be achieved by an expansion of chain dimension such that most of the protein is at least partially exposed to solvent. However, the denatured protein may still be left with “residual” hydrophobic interactions involving small nonpolar contacting modules that

are partially exposed to solvent [Figs. 5(B) and 5(C)]. Some of these contacts are fluctuating; and, they may be between modules that form parts of amino acid residue pairs that are local or nonlocal along the chain sequence. Inasmuch as the aqueous environment of these nonpolar contacts can be typified by methane–methane and even methane–neopentane PMFs, they would not be destabilized by urea [Figs. 2 and 3(A)]. Hence, increasing the concentration of urea would not lead to further significant expansion of the urea-denatured chains. The present consideration is agnostic about whether the residual interactions are native-like or nonnative.

The compactness of heat-denatured states may be similarly rationalized by Figure 4(B). First, because $\Delta C_p \approx 0$ for a contacting methane pair, it is possible for the ΔC_p signature of a compact denatured state with partial solvent exposure [cf. Figs. 5(B) and 5(C)] to be similar to that of a hypothetical random-coil state with full solvent exposure. This scenario³⁷ is apparently consistent with the experiments of Nishii et al.,⁶² who determined ΔC_p as a function of R_g for native and various denatured (nonnative) states of apomyoglobin and ferricytochrome *c*. They found that when a protein's R_g is reduced from that of its chemical-denatured states, initially there is little change in ΔC_p . Most of the ΔC_p change occurs as a sharp decrease when R_g becomes sufficiently close to its native value. This ΔC_p “retardation”⁶² may now be understandable if the hydrophobic interactions in partially solvated compact denatured proteins are similar to the two-methane contact interactions in Figure 4(B). In that case, the ΔC_p of the protein is expected to be similar to that of a hypothetical random-coil state until water is squeezed out at the final formation stages of the protein's hydrophobic core. Only at that point would ΔC_p decrease sharply as it crosses over from “pair” to “bulk” behavior. Size dependence may come into play in this crossover as well, since there are indications that pairwise association of hydrophobic solutes several times bigger than methane may have $\Delta C_p < 0$.⁶³ Second, $\Delta C_p \approx 0$ for a methane–methane contact implies that the enthalpy and entropy of such a pairwise interaction do not vary much with temperature. Simulations show that the overall favorability of this pair interaction ($\Delta G < 0$) is the result of a stabilizing entropic component ($\Delta S > 0$) that overcompensates for a destabilizing enthalpic contribution ($\Delta H > 0$).^{36–38} Therefore, insofar as the compactness of heat-denatured states are maintained by hydrophobic interactions typified by that of methane pairs, $\Delta C_p \approx 0$ of these pairwise interactions implies that an increase in temperature T of an already heat-denatured protein would not cause it to further expand because the Boltzmann weight of the methane pair interaction $\exp(-\Delta G/k_B T) = \exp(-\Delta H/k_B T + \Delta S/k_B)$ (where k_B is Boltzmann's constant) does not decrease with increasing T .

CONCLUSIONS

Atomic simulations of size and spatial dependence of pairwise nonpolar interactions presented led to a rudimentary physical picture of residual hydrophobic interactions

in protein denatured states. This perspective rationalizes several intriguing phenomena that are puzzling from a bulk-phase transfer/SASA view. Inspired by earlier solvent-exchange⁶⁴ and preferential interaction¹² concepts of urea denaturation, we also applied a Kirkwood–Buff approach⁶⁵ to relate nonpolar interactions to structural aspects of the aqueous urea solvent. Mechanisms for urea-modulated pairwise hydrophobic effects are found to be consistent with that of preferential interaction.¹² Details of this latter investigation will be reported elsewhere.

ACKNOWLEDGMENTS

The authors thank Robert L. Baldwin and Clare Woodward for their critical reading of an earlier version of the article, Bruce Bowler, Julie Forman-Kay, Yuji Goto, George Makhatadze, Kevin Plaxco, Régis Pomès, Jim Rini, Jose Sanchez-Ruiz, David Shortle, Maria-Luisa Tasayco, and Dev Thirumalai for helpful discussions, and Danny Heap for his effort in maintaining our computing system. This work was supported in part by Canadian Institutes of Health Research (CIHR) Grant MOP-15323. H.S.C. is a Canada Research Chair in Biochemistry.

REFERENCES

1. Kauzmann W. Some factors in the interpretation of protein denaturation. *Adv Protein Chem* 1959;14:1–63.
2. Tanford C. Protein denaturation. *Adv Protein Chem* 1970;24:1–95.
3. Myers JK, Pace CN, Scholtz JM. Denaturant *m*-values and heat capacity changes: Relation to changes in accessible surface area of protein unfolding. *Protein Sci* 1995;4:2138–2148.
4. Makhatadze GI. Thermodynamics of protein interactions with urea and guanidinium hydrochloride. *J Phys Chem B* 1999;103:4781–4785.
5. Nozaki Y, Tanford C. Solubility of amino acids and related compounds in aqueous urea solutions. *J Biol Chem* 1963;238:4074–4081.
6. Wetlaufer DB, Malik SK, Stoller L, Coffin RL. Nonpolar group participation in denaturation of proteins by urea + guanidinium salts. Model compound studies. *J Am Chem Soc* 1964;86:508–514.
7. Kresheck GC, Benjamin L. Calorimetric studies of hydrophobic nature of several protein constituents and ovalbumin in water and in aqueous urea. *J Phys Chem* 1964;68:2476–2486.
8. Roseman M, Jencks WP. Interactions of urea and other polar compounds in water. *J Am Chem Soc* 1975;97:631–640.
9. Nandi PK, Robinson DR. Effects of urea and guanidine-hydrochloride on peptide and nonpolar groups. *Biochemistry* 1984;23:6661–6668.
10. Zou Q, Habermann-Rottinghaus SM, Murphy KP. Urea effects on protein stability: Hydrogen bonding and the hydrophobic effect. *Proteins* 1998;31:107–115.
11. Liu Y, Bolen DW. The peptide backbone plays a dominant role in protein stabilization by naturally-occurring osmolytes. *Biochemistry* 1995;34:12884–12891.
12. Prakash V, Loucheux C, Scheufele S, Gorbunoff MJ, Timasheff SN. Interactions of proteins with solvent components in 8M urea. *Arch Biochem Biophys* 1981;210:455–464.
13. Scholtz JM, Barrick D, York EJ, Stewart JM, Baldwin RL. Urea unfolding of peptide helices as a model for interpreting protein unfolding. *Proc Natl Acad Sci USA* 1995;92:185–189.
14. Courtenay ES, Capp MW, Saecker RM, Record MT. Thermodynamic analysis of interactions between denaturants and protein surface exposed on unfolding: Interpretation of urea and guanidinium chloride *m*-values and their correlation with changes in accessible surface area (ASA) using preferential interaction coefficients and the local-bulk domain model. *Proteins* 2000;41(S4):72–85.
15. Crippen GM. A Gaussian statistical mechanical model for the equilibrium thermodynamics of barnase folding. *J Mol Biol* 2001;306:565–573.

16. Dill KA, Shortle D. Denatured states of proteins. *Annu Rev Biochem* 1991;60:795–825.
17. Neri D, Billeter M, Wider G, Wüthrich K. NMR determination of residual structure in a urea-denatured protein, the 434-repressor. *Science* 1992;257:1559–1563.
18. Saab-Rincon G, Gualfetti PJ, Matthews CR. Mutagenic and thermodynamic analyses of residual structure in the alpha subunit of tryptophan synthase. *Biochemistry* 1996;35:1988–1994.
19. Klein-Seetharaman J, Oikawa M, Grimshaw SB, Wirmer J, Duchardt E, Ueda T, Imoto T, Smith LJ, Dobson CM, Schwalbe H. Long-range interactions within a nonnative protein. *Science* 2002;295:1719–1722.
20. Shortle D, Ackerman MS. Persistence of native-like topology in a denatured protein in 8 M urea. *Science* 2001;293:487–489.
21. Plaxco KW, Gross M. Unfolded, yes, but random? Never! *Nature Struct Biol* 2001;8:659–660.
22. Baldwin RL. Protein folding—Making a network of hydrophobic clusters. *Science* 2002;295:1657–1658.
23. Alonso DOV, Dill KA. Solvent denaturation and stabilization of globular proteins. *Biochemistry* 1991;30:5974–5985.
24. Millet IS, Townsley LE, Chiti F, Doniach S, Plaxco KW. Equilibrium collapse and the kinetic “foldability” of proteins. *Biochemistry* 2002;41:321–325.
25. Wood RH, Thompson PT. Differences between pair and bulk hydrophobic interactions. *Proc Natl Acad Sci USA* 1990;87:8921–8927.
26. Chan HS, Dill KA. Solvation: How to obtain microscopic energies from partitioning and solvation experiments. *Annu Rev Biophys Biomol Struct* 1997;26:425–459.
27. Karplus M. Biophysical discussion. *Biophys J* 1980;32:45–46.
28. Kim PS, Baldwin RL. Specific intermediates in the folding reactions of small proteins and the mechanism of protein folding. *Annu Rev Biochem* 1982;51:459–489.
29. Pratt LR, Chandler D. Theory of hydrophobic effect. *J Chem Phys* 1977;67:3683–3704.
30. Lum K, Chandler D, Weeks JD. Hydrophobicity at small and large length scales. *J Phys Chem B* 1999;103:4570–4577.
31. Southall NT, Dill KA, Haymet ADJ. A view of the hydrophobic effect. *J Phys Chem B* 2002;106:521–533.
32. Geiger A, Rahman A, Stillinger FH. Molecular-dynamics study of the hydration of Lennard–Jones solutes. *J Chem Phys* 1979;70:263–276.
33. Pangali C, Rao M, Berne BJ. Hydrophobic hydration around a pair of apolar species in water. *J Chem Phys* 1979;71:2982–2990.
34. Hummer G, Garde S, García AE, Paulaitis ME, Pratt LR. Hydrophobic effects on a molecular scale. *J Phys Chem B* 1998;102:10469–10482.
35. Sorenson JM, Hura G, Soper AK, Pertsemlidis A, Head-Gordon T. Determining the role of hydration forces in protein folding. *J Phys Chem B* 1999;103:5413–5426.
36. Shimizu S, Chan HS. Temperature dependence of hydrophobic interactions: A mean force perspective, effects of water density, and nonadditivity of the thermodynamic signatures. *J Chem Phys* 2000;113:4683–4700. [Erratum: *J Chem Phys* 2002;116:8636.]
37. Shimizu S, Chan HS. Configuration-dependent heat capacity of pairwise hydrophobic interactions. *J Am Chem Soc* 2001;123:2083–2084.
38. Ghosh T, García AE, Garde S. Enthalpy and entropy contributions to the pressure dependence of hydrophobic interactions. *J Chem Phys* 2002;116:2480–2486.
39. Wallqvist A, Covell DG, Thirumalai D. Hydrophobic interactions in aqueous urea solutions with implications for the mechanism of protein denaturation. *J Am Chem Soc* 1998;120:427–428.
40. Ikeguchi M, Nakamura S, Shimizu K. Molecular dynamics study on hydrophobic effects in aqueous urea solutions. *J Am Chem Soc* 2001;123:677–682.
41. Jorgensen WL. BOSS, Version 4.1. New Haven, CT: Yale University; 1999.
42. Kuharski RA, Rossky PJ. Molecular-dynamics study of solvation in urea water solution. *J Am Chem Soc* 1984;106:5794–5800.
43. Shimizu S, Chan HS. Anti-cooperativity in hydrophobic interactions: A simulation study of spatial dependence of three-body effects and beyond. *J Chem Phys* 2001;115:1414–1421.
44. Shimizu S, Chan HS. Anti-cooperativity and cooperativity in hydrophobic interactions: Three-body free energy landscapes and comparison with implicit-solvent potential functions for proteins. *Proteins* 2002;48:15–30. [Erratum: *Proteins* 2002;49:294.]
45. Smith PE. Computer simulation of cosolvent effects on hydrophobic hydration. *J Phys Chem B* 1999;103:525–534.
46. Muller N. A model for the partial reversal of hydrophobic hydration by addition of a urea-like cosolvent. *J Phys Chem* 1990;94:3856–3859.
47. Graziano G. On the solubility of aliphatic hydrocarbons in 7 M aqueous urea. *J Phys Chem B* 2001;105:2632–2637.
48. Makhatadze GI, Privalov PL. Energetics of protein structure. *Adv Protein Chem* 1995;47:307–425.
49. Zhou HX. A Gaussian-chain model for treating residual charge–charge interactions in the unfolded state of proteins. *Proc Natl Acad Sci USA* 2002;99:3569–3574.
50. Kaya H, Chan HS. Towards a consistent modeling of protein thermodynamic and kinetic cooperativity: How applicable is the transition state picture to folding and unfolding? *J Mol Biol* 2002;315:899–909.
51. Sosnick TR, Trehwella J. Denatured states of ribonuclease A have compact dimensions and residual secondary structure. *Biochemistry* 1992;31:8329–8335.
52. Hagihara Y, Hoshino M, Hamada D, Kataoka M, Goto Y. Chain-like conformation of heat-denatured ribonuclease A and cytochrome c as evidenced by solution X-ray scattering. *Fold Des* 1998;3:195–201.
53. Miller WG, Goebel CV. Dimensions of protein random coils. *Biochemistry* 1968;7:3925–3935.
54. Choy WY, Forman-Kay JD. Calculation of ensembles of structures representing the unfolded state of an SH3 domain. *J Mol Biol* 2001;308:1011–1032.
55. Choy WY, Mulder FAA, Crowhurst KA, Muhandiram DR, Millett IS, Doniach S, Forman-Kay JD, Kay LE. Distribution of molecular size within an unfolded state ensemble using small-angle X-ray scattering and pulse field gradient NMR techniques. *J Mol Biol* 2002;316:101–112.
56. Shortle D. Composites of local structure propensities: Evidence for local encoding of long-range structure. *Protein Sci* 2002;11:18–26.
57. Pappu RV, Srinivasan R, Rose GD. The Flory isolated-pair hypothesis is not valid for polypeptide chains: Implications for protein folding. *Proc Natl Acad Sci USA* 2000;97:12565–12570.
58. Barber MN, Ninham BW. Random and Restricted Walks. New York: Gordon & Breach; 1970.
59. Feldman HJ, Hogue CWV. Probabilistic sampling of protein conformations: New hope for brute force? *Proteins* 2002;46:8–23.
60. Dill KA. Theory for the folding and stability of globular-proteins. *Biochemistry* 1985;24:1501–1509.
61. Arai M, Kuwajima K. Role of the molten globule state in protein folding. *Adv Protein Chem* 2000;53:209–282.
62. Nishii I, Kataoka M, Tokunaga F, Goto Y. Cold denaturation of the molten globule states of apomyoglobin and a profile for protein-folding. *Biochemistry* 1994;33:4903–4909.
63. Christian SD, Tucker EE. Importance of heat capacity effects in the association of hydrophobic moieties in aqueous solution. *J Sol Chem* 1982;11:749–754.
64. Schellman JA. Selective binding and solvent denaturation. *Biopolymers* 1987;26:549–559.
65. Kirkwood JG, Buff FP. The statistical mechanical theory of solutions. 1. *J Chem Phys* 1951;19:774–777.